ELSEVIER

Cement & Concrete Composites 26 (2004) 473–479

Cement & Concrete Composites

www.elsevier.com/locate/cemconcomp

Experimental investigation into early age shrinkage of cement paste by using fibre Bragg gratings

Volker Slowik *, Evelyn Schlattner, Thomas Klink

Leipzig University of Applied Sciences, PF 66, D-04251 Leipzig, Germany

Abstract

A new technique based on fibre optics has been utilised for investigating early age shrinkage of cement paste. Fibre Bragg gratings are strain sensors within optical fibres which were embedded here in cement paste specimens. In this way, shrinkage strains could be measured starting from the beginning of the setting. Sufficient bond strength between the sensor fibre and the surrounding early age cement paste has been proved in pull-out tests. Influences of the w/c-ratio, the curing conditions as well as the specimen geometry were under investigation in the experiments. The significant influence of the drying conditions on the shrinkage strain during the first day after casting is demonstrated. Whereas the early age shrinkage appeared to result in a rather uniform deformation the subsequent drying shrinkage caused significant strain gradients in the specimens.

Keywords: Early age concrete; Early age shrinkage; Cement paste; Fibre Bragg gratings; Fibre sensors

1. Introduction

Measuring shrinkage strains of cement paste at early age, i.e. between 0 and 12 h after mixing, appears to be difficult from the practical point of view since strain or displacement gauges cannot be attached before a certain minimum strength has been reached. Therefore, most shrinkage strains referred to in the literature have been measured starting from the time of demoulding [1] and technical standards or recommendations [2] for determining such quantities are based on a certain age for starting the shrinkage measurement. There are, however, methods for determining the volume change of cementitious materials in the plastic stage, for instance those based on measuring the settlement of fresh mortar in a tapered, i.e. cone-shaped, form [3]. But such methods do not provide the opportunity to continuously monitor the shrinkage from the plastic through the hardened stage of the material.

Although the shrinkage strain up to an age of about 1 day is not subject of "conventional" material testing it does have its practical importance. A major problem in the concrete floor technology is the early age cracking due to shrinkage of the young concrete. It is caused mainly by the capillary water transport out of the hardening concrete. The resulting cracks are located on the concrete surface and appear usually within the first 24 h after casting. Although appropriate curing is an important part of state-of-the-art concrete technology, early age cracking is still one of the most common structural faults.

The intention of the work presented here was to contribute into a better understanding of early age shrinkage by using a fairly new technology, the fibre Bragg gratings (FBGs). Because of the quite complex experimental set-up and the comparably high sensor price the presented technique is not proposed as a new standard method for shrinkage tests but might be useful for answering certain questions in concrete research and development.

2. Measuring technique

Initially, in-line FBGs were developed as frequency filters for optical telecommunication systems. Their usability for measuring strains appeared to be an

* Corresponding author. Tel.: +49-341-3076-6261; fax: +49-341-3076-7045.

E-mail address: slowik@fbb.htwk-leipzig.de (V. Slowik).

0958-9465/$ - see front matter © 2003 Elsevier Ltd. All rights reserved.
doi:10.1016/S0958-9465(03)00077-5

additional result of this development. In 1989, Meltz et al. [4] produced FBGs by "writing" a series of equidistant lines into the glass core of a standard single-mode telecommunication fibre. For this writing process the interference pattern of two laser beams has been used. The equidistant lines forming the Bragg grating are characterised by a refraction index different from the one of the regular fibre core. Light propagating in the glass fibre core will be reflected by the interfaces between the regions having different refraction indices. The reflected light is generally out of phase and tends to cancel. However, for a certain wavelength, the Bragg wavelength, the light reflected by the periodically varying refraction index will be in equal phase and amplified [5]. This results in a characteristic peak at this wavelength in the transmission as well as in the reflection spectrum, see Fig. 1. Since the peak wavelength depends on the spacing of the lines forming the grating the latter can be used for measuring strains. If the optical fibre is stretched, the Bragg wavelength increases.

It has to be taken into account that the Bragg wavelength depends on the temperature too. The Bragg wavelength shift $\Delta\lambda$ is related to the strain ε and to the temperature change ΔT by

$$\frac{\Delta\lambda}{\lambda} = (1 - p_e) \cdot \varepsilon + \xi \cdot \Delta T$$

where p_e and ξ are the strain-optical and the thermo-optical coefficients, respectively. Once these coefficients are known for a specific type of FBG sensor, the method is calibration free and allows long-term measurements without a "drift" of the strain readings. For a known temperature, the thermo-optical effect can be compensated analytically as done in the experiments presented here. Because of the excellent long-term stability of the strain measurements the FBG sensors may be used efficiently for structural monitoring [6–8]. Furthermore, the small dimensions of FBG allow its utilisation for "microsensors" opening new fields of application in material science.

3. Experiments

Prismatic cement paste specimens having the dimensions of $9 \times 3 \times 3$ cm^3 were cast into a form made of a sponge-like and very flexible foamed polyvinylchloride, Fig. 2. The low stiffness of the form was intended to allow unhindered shrinkage of the sample. The glass fibre containing a FBG sensor has been embedded parallel to the longitudinal axis of the specimen with the actual sensitive part (FBG) located in the middle section. If not stated otherwise, the sensor fibre was placed in the centre axis of the specimen. A layer of impermeable plastic film placed between the form and the cement paste served for preventing water transport into the form. In some of the specimens, drying was possible on the upper surface, other specimens were sealed completely. For compensating the thermo-optical effect, all specimens had been equipped with internal thermocouples. In all test series, a Portland cement CEM I 42.5 R was used.

The optical communication fibre utilised consists of a glass core with 9 μm diameter where the light is propagating. This core is surrounded by a stabilising glass cladding with a diameter of 125 μm. For further protection an acrylic coating with a diameter of 245 μm is applied to the fibre. In the experiments presented here, the coating has been removed from the fibre over a length of about 20 mm in the vicinity of the FBG sensor. By this measure, the bond strength between the sensor and the surrounding cement paste was increased.

The shrinkage measurement was quasi-feedback free, i.e. there was no significant hindrance of the shrinkage strain by the sensor itself. This is due to the low uniaxial stiffness of the fibre being about 1000 times smaller than the one of the hardening cement paste sample if its modulus of elasticity is assumed to be 1000 N/mm^2 and its whole cross-sectional area is taken into account. However, sufficient bond between fibre and hardening cement paste is a precondition for the correct shrinkage measurement. In order to look deeper into this problem

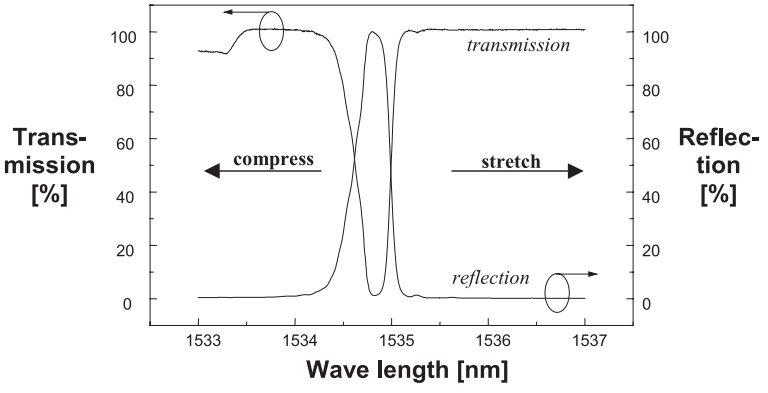

Fig. 1. Transmission and reflection spectrum for a fibre Bragg grating.

Fig. 2. Cement paste specimen in form, sensor fibre and optical adapters.

fibre pull-out tests with hardening cement paste have been performed [9]. Several fibres were embedded over a length of 40 mm in the same cement paste sample and pulled out under displacement control (0.05 mm/s) at different age. The obtained load–displacement curves are shown in Fig. 3. Already at an age of 6 h a typical bond-slip behaviour was observed. According to accompanying needle penetration tests (Vicat tests) the begin of setting was at an age of 5 h under the specific test conditions. (It should be noted that in the actual shrinkage tests the hardening process was faster, probably because of different thermal conditions.) Finite Element analyses of the pull-out test as well as of the actual shrinkage test [9] revealed that in both cases significant bond stresses occur only within a contact length of about 2 mm from the cement paste surface which is roughly eight times the fibre diameter and in good accordance with technical rules valid for anchoring problems. For a shrinkage strain of −700 μm/m the bond stresses in the shrinkage test are smaller than the bond strength found in the pull-out tests at an age of 6 h. Even if the bond strength would be reached in the shrinkage tests at the end faces of the sample there would be a remaining grip length of more than 40 mm on both sides of the sensor for transferring the axial load into the fibre. It is concluded that the fibre sensors embedded in the cement paste samples are applicable for measuring the early age shrinkage strain. A slip between the fibre and the surrounding matrix does not occur due to the low fibre stiffness and the long grip length when compared to the fibre diameter.

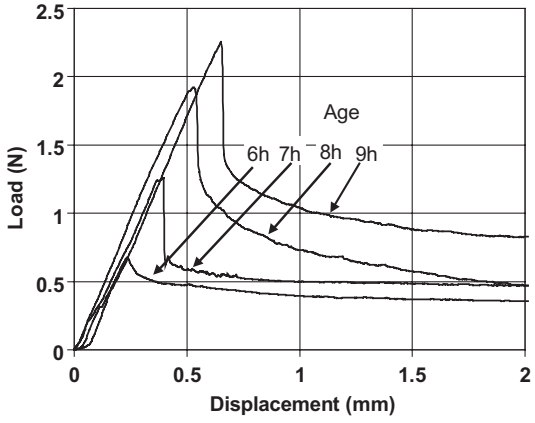

Fig. 3. Load–displacement diagrams from fibre pull-out tests at different age.

4. Experimental observations and discussion

Fig. 4 shows a characteristic shrinkage curve obtained for a water–cement ratio of 0.45. In all presented diagrams the age is related to the moment of mixing the cement paste components. About 3h after mixing, shrinkage starts and strongly increases until an age of

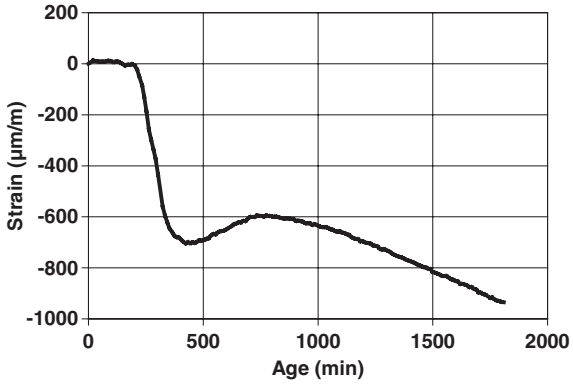

Fig. 4. Characteristic early age shrinkage curve for cement paste.

about 6 h is reached. This is the time period between the beginning and the end of the setting. Simultaneously performed needle penetration tests confirmed this assumption. If there would be a volume change of the fresh cement paste already before the beginning of the setting, for instance due to separation of the components, it probably could not be monitored by the method used here due to insufficient bond. The comparably high early age shrinkage strain at the age between about 3 and 6 h is assumed to be mainly caused by the capillary transport of water towards the specimen surface. The resulting negative hydrostatic pressure in the capillaries causes additional internal forces between the particles and consequently shrinkage, referred to as capillary shrinkage or plastic shrinkage. In addition, chemical shrinkage occurs which, however, is not predominant for the w/c-ratios used here.

After the period characterised by the high shrinkage strains, a volume increase is observed. This is predominantly caused by thermal strains. Using embedded thermo-couples a temperature increase by 10–15 K could be determined at this age explaining the observed positive strain. The subsequent drying shrinkage strain yielded toward a final value, see Fig. 5. After 12 days the total strain amounted to about −2700 μm/m for 20 °C and 40% air humidity. If the strain measurement would have been started at an age of 24 h, i.e. after demoulding in "conventional" tests, the early age shrinkage could not have been captured resulting in a value of −2000 μm/m after 12 days. The drying shrinkage of the hardened cement paste is caused by the evaporation of the pore water.

As already stated before, the measured shrinkage strain includes the effect of thermal expansion. Since the coefficient of thermal expansion of the hardening cement paste is not known and continuously changing in the early age it appears to be too speculative to separate both effects on the basis of the experimental results.

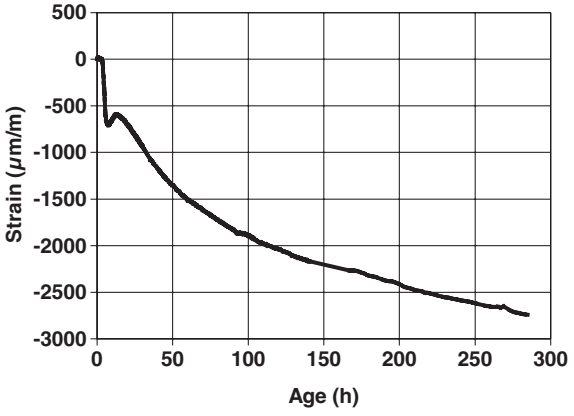

Fig. 5. Characteristic shrinkage curve for cement paste, same sample as in Fig. 4.

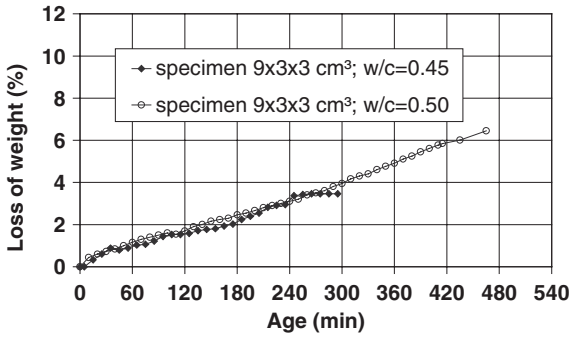

Fig. 6. Loss of weight versus time for early age cement paste.

The total water loss at the early age was determined by measuring the weight of the specimens. Fig. 6 shows the results obtained for two of the samples with different w/c-ratios. In contrary to the measured early age shrinkage strains, the water loss appears to be nearly linear and starts right after the mixing of the components. In the fresh cement paste, the water loss is caused by separation and evaporation of water at the specimen surface. This process does not necessarily result in a multi-axial contraction of the specimen.

Fig. 7 shows a strain–time curve which has been measured after a re-saturation of one of the samples. The specimen has been subjected to drying at its upper surface for 16 days while it was still within the form, see Fig. 2. Afterwards, water has been applied to the surface. Within a few minutes a strain of about 300 μm/m was measured. Subsequently, the strain increased asymptotically towards a value of about 1200 μm/m which equals nearly two thirds of the total shrinkage strain value reached before moistening the specimen. It is demonstrated that a major portion of the drying shrinkage is reversible.

As far as the influence of the w/c-ratio is concerned inconsistent results were obtained. Fig. 8 shows the early age shrinkage curves obtained for different w/c-ratios. All the shrinkage curves presented in the same diagram were measured in parallel, i.e. at the same time for

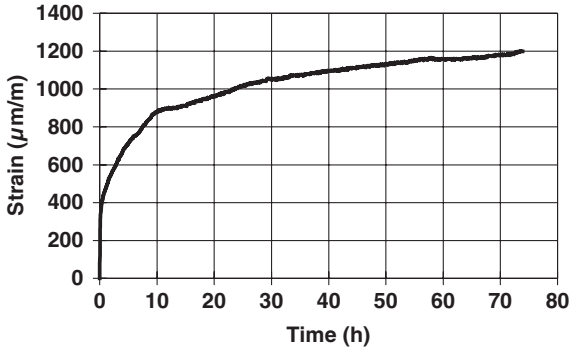

Fig. 7. Strain–time curve measured after re-moistening a cement paste sample (age 16 days, specimen size $9 \times 3 \times 3$ cm^3, w/c = 0.45).

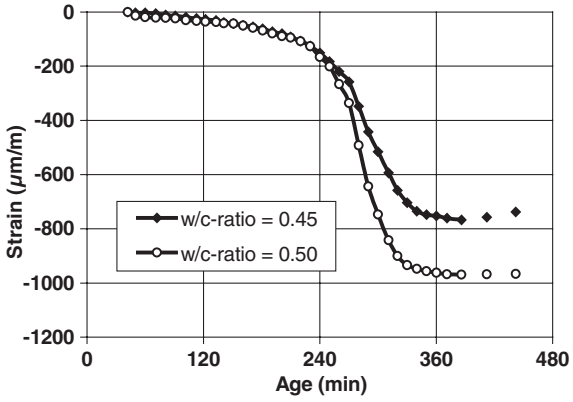

Fig. 8. Shrinkage curves for cement paste with different w/c-ratios (specimen size $9 \times 3 \times 3$ cm^3).

samples made of the same batch. As can be seen in Fig. 8, the early age shrinkage strain value is higher for the sample with the higher w/c-ratio which can be explained by the larger water volume available. In another test series, see Fig. 9, a different observation was made. For a w/c-ratio of 0.5 the early age shrinkage is significantly reduced as compared to the w/c-ratio of 0.45. In fact, the early age shrinkage is nearly completely compensated by the thermal expansion. This observation is explained by a water layer formed at the upper surface of the specimen with $w/c = 0.5$ providing a perfect curing and preventing capillary water transport out of the specimen. The same effect, i.e. a reduced early age shrinkage with increasing w/c-ratio, has been reported in the literature before [1,10]. For the two test series showing contradictory results cement of different batches was used. Early age shrinkage appears to be a complex process being very sensitive to small changes in the material composition and in the environmental conditions. This corresponds to practical experiences in concrete technology where the probability of early age cracks is not easy to predict resulting occasionally in corresponding problems.

For obtaining a better understanding of the phenomena causing early age shrinkage, in some of the tests

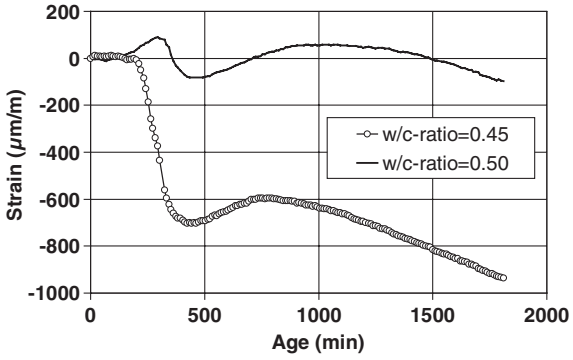

Fig. 9. Shrinkage curves for cement paste with different w/c-ratios (specimen size $9 \times 3 \times 3$ cm^3, different cement as used for Fig. 8).

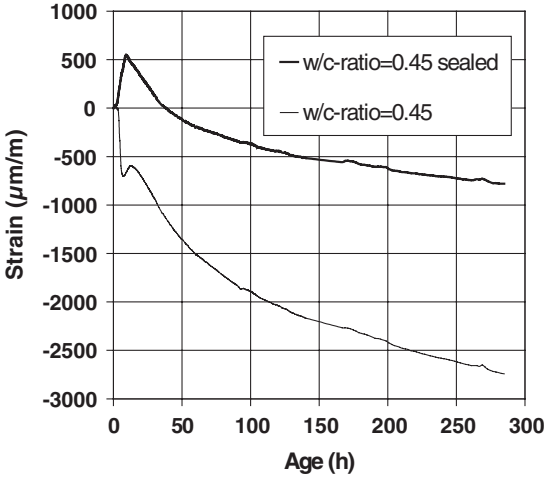

Fig. 10. Shrinkage curves for a sealed and unsealed cement paste sample, respectively (specimen size $9 \times 3 \times 3$ cm^3).

the surface of the sample was sealed in order to prevent the water transport out of the specimen. On the specimen top face, an impermeable plastic film was glued to the others covering the side faces of the form, see Section 3. Fig. 10 shows the shrinkage curves for a completely sealed specimen and for one with an open upper surface, Fig. 11 the corresponding temperature curves. As expected, the shrinkage strain is significantly lower in the sealed specimen where the capillary shrinkage does not occur. The early age shrinkage strain was even overcompensated by the thermal expansion. The negative strain observed results from chemical shrinkage. Because of the water evaporation at the open surface and no thermal insulation by a sealing layer the temperature in the specimen with open surface was not as high as in the sealed specimen. Furthermore, the w/c-ratio appears to have no significant influence on the temperature curve.

Fig. 12 shows the influence of an air current applied to the open surface for accelerating the water evaporation. Two specimens with different w/c-ratios were subjected to the air current, two other specimens were not.

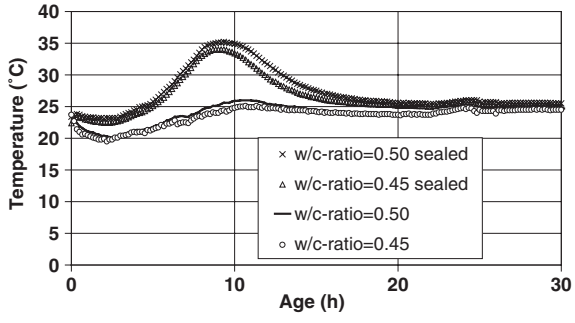

Fig. 11. Temperature curves for a sealed and unsealed cement paste sample, respectively (specimen size $9 \times 3 \times 3$ cm^3, same samples as in Fig. 10).

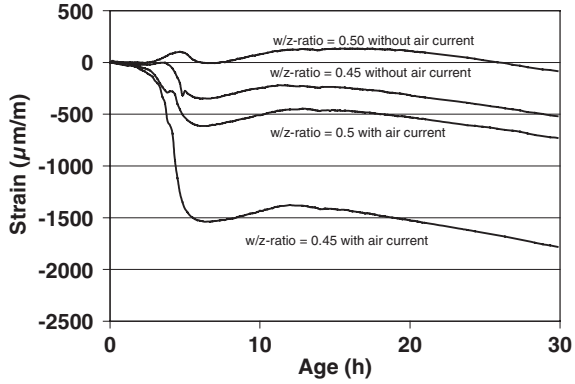

Fig. 12. Shrinkage curves as dependent on the w/c-ratio and on the drying conditions (specimen size $9 \times 3 \times 3$ cm^3).

The curves clearly demonstrate that the drying conditions do have a major influence on the early age shrinkage. For a w/c-ratio of 0.45 and the air current applied −1500 μm/m were measured after about 6 h. As already found in another test series, for a w/c-ratio of 0.5 smaller shrinkage strain values were measured as compared to a w/c-ratio of 0.45.

Shrinkage strains generally depend on the specimen geometry as well as on the location and orientation within the specimen. Whereas in the tests reported so far the specimen size was always $9 \times 3 \times 3$ cm^3, in a special test series two different specimen sizes were used. One of them was the standard size mentioned above, the other one was $9 \times 3 \times 6$ cm^3. In each of the specimens a FBG sensor was located longitudinally in the centre axis of the sample. Fig. 13 shows the obtained shrinkage curves. It was found that the early age shrinkage (within the first 6 h) is nearly independent of the specimen size whereas the drying shrinkage is faster in the small specimen. The capillary or plastic shrinkage results from capillary water transport to the specimen surface. At this age, the permeability of the cement paste is much higher as compared to the one of the hardened cement paste. Therefore, the distance to the specimen surface is not as important for the water transport as in the case of

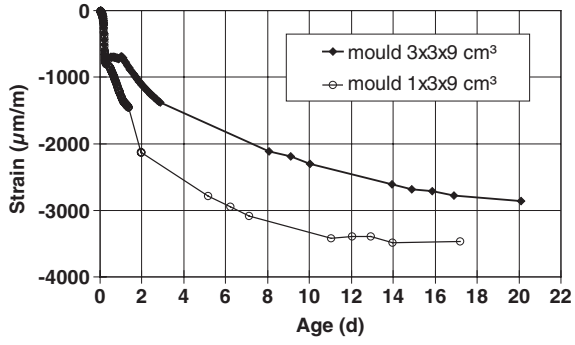

Fig. 13. Shrinkage curves for different specimen sizes (w/c = 0.45, sensor located in the centre).

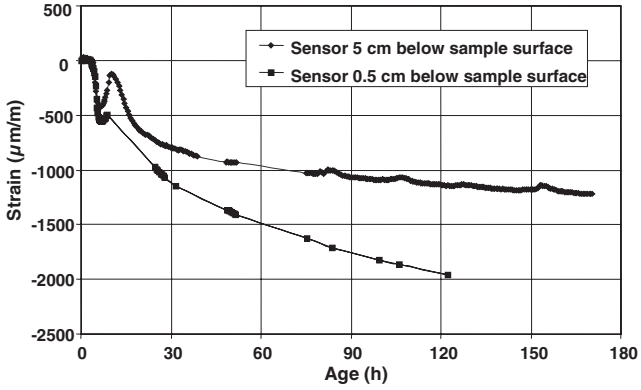

Fig. 14. Shrinkage strain as dependent on the location of the sensor (w/c = 0.45, specimen size $9 \times 3 \times 6$ cm^3).

hardened cement paste. In the latter, the low permeability leads to strain gradients and size dependent drying. In Fig. 13 it can be seen that the shrinkage strain difference is high at the age between 4 and 12 days, but seems to decrease with the age afterwards. Eventually, for both specimens the shrinkage strain should reach the same final value.

Because of the high permeability of the early age cement paste it is expected that the capillary shrinkage does not result in a significant strain gradient. This assumption could be confirmed experimentally. A specimen with the size $9 \times 3 \times 6$ cm^3 was cast and two FBG sensors were embedded at different distances from the surface, 5 and 0.5 cm, respectively. In the first hours after mixing, the strain values seem to be independent of the sensor location, see Fig. 14. However, after about 1 day, the strains measured closer to the surface are changing faster than those measured by the inner sensor. This means that a strain gradient started to develop at an age of about 1 day. The early age shrinkage, apparently, did not result in a significant strain gradient for this specimen size.

5. Conclusions

The FBG sensors have proven useful for investigating early age shrinkage of cementitious materials. Without these sensors, obtaining some of the experimental results presented would have required considerably greater efforts. With the proposed experimental technique, it is now possible to systematically investigate different influences on the shrinkage process as well as the effect of shrinkage reducing agents. However, because of the expenses for the FBGs the proposed technique may not be recommended as a standard method in material testing.

The magnitude of early age shrinkage is very sensitive to small changes in the material composition. As far as the influence of the w/c-ratio is concerned, contradictory results were obtained for different cement batches. The

significant influence of the drying conditions on the early age shrinkage could be clearly demonstrated by applying an air current to the surface of the specimens.

The early age shrinkage, i.e. within the first day, did not cause significant strain gradients in the specimens, the subsequent drying shrinkage did. The reason for this difference is the higher water permeability of the cement paste in its plastic stage.

Acknowledgement

The financial support of the project by the German Research Department (Bundesministerium für Bildung und Forschung) is gratefully acknowledged.

References

[1] Grube H. Ursachen des Schwindens von Beton und Auswirkungen auf Betonbauteile. Forschungsinstitut der Zementindustrie. Schriftenreihe der Zementindustrie 1991;52.

[2] DIN 52450, German Standard. Bestimmung des Schwindens und Quellens an kleinen Probekörpern, August 1985.

[3] Greim M, Teubert O. Vorrichtung zur Erfassung des frühen Dehn- und Schwindverhaltens von Baustoffen. German Patent DE 10046284 A1, 28 March 2002.

[4] Meltz G, Morey WW, Glenn WH. Formation of Bragg-gratings in optical fibers by a transverse holographic method. Opt Lett 1989;14(15):823–5.

[5] Melle SM, Liu K, Measures R. Practical fiber-optic Bragg grating strain gauge system. Appl Opt 1993;32(19):3601–9.

[6] Sirkis JS. Using Bragg grating sensor systems in construction materials and bridges: perspectives and challenges. In: Ansari F, editor. Proceedings of the International Workshop on Fiber Optic Sensors for Construction Materials and Bridges, Newark, NJ, USA. Lancaster: Technomic Publishing Company; 1998. p. 44–61.

[7] Saouma VE, Anderson DZ, Ostrander K, Lee B, Slowik V. Application of fiber Bragg grating in local and remote infrastructure health monitoring. Mater Struct 1998;31:259–66.

[8] Schlattner E, Slowik V, Klink T. Neue Möglichkeiten zur langzeitigen Dehnungsmessung im Bauwesen mittels Faser–Bragg–Gitter–Sensoren. Bautechnik 1999;76(10):884–7.

[9] Slowik V, Schlattner E, Klink T. Faser–Bragg–Sensoren in Bauwerken. Research Report, Leipzig University of Applied Sciences, 1999.

[10] Wittmann FH. Zur Ursache der sogenannten Schrumpfrisse. Zement und Beton 1975;85:10–6.